vertebrate or bacterial DNA [20,21]. RLRs are also involved in sensing cytoplasmic DNA [22,23]. Chen and colleagues have shown that DNA viruses can activate RIG-I pathway via RNA polymerase III [24]. Unlike RLRs, the DAI, IFI16, DDX41, and cGAS DNA sensors require the adaptor molecule STING to induce Type I IFN expression [19,25,26]. STING localizes to the ER and requires TBK1 to induce Type I IFN expression [19].

The protein kinase TBK1 is essential for Type I IFN expression in response to cytoplasmic DNA [27]. Ser-172 of TBK1 is autophosphorylated in its activation loop, and autophosphorylation is essential for triggering TBK1-dependent signaling [28]. Active TBK1 phosphorylates the transcription factor IRF-3, leading to relocalization of IRF-3 from cytoplasm to nucleus [29]. Recently, we showed that phospho-TBK1 (p-TBK1) localizes on mitochondria in response to cytoplasmic hepatitis C virus RNA [30]; however, it is unclear where TBK1 localizes in response to cytoplasmic viral DNA. Here, we used an anti-p-TBK1 specific antibody to determine the subcellular localization of p-TBK1 in response to cytoplasmic viral DNA. We elucidated the cell type-specific subcellular localization of p-TBK1 in response to cytoplasmic viral DNA.

Results

Localization of p-TBK1 on mitochondria in HeLa cells

We used anti-TBK1 (total TBK1) and anti-p-TBK1 antibodies to detect total TBK1 and p-TBK1 expression by western blotting and immunofluorescence microscopy analyses. Exogenous expression of RIG-I CARDs, TICAM-1, IPS-1, or STING induces the activation of downstream signaling without stimulation [4,14,26,31]. We found that exogenous expression of RIG-I CARDs, TICAM-1, IPS-1, or STING induced TBK1 phosphorylation, whereas total TBK1 levels were not affected (Figure 1A). We investigated the subcellular localization of p-TBK and total TBK1. Total TBK1 was dispersed through the cytoplasm, whereas p-TBK1 exhibited mitochondrial localization in HeLa cells that expressed RIG-I CARDs, IPS-1, or STING (Figure 1B and 1C). More than 70 % of p-TBK1 induced by RIG-I CARDs, IPS-1, or STING expression showed mitochondrial localization (Figure 1B). In contrast, p-TBK1 did not show mitochondrial localization in HeLa cells that expressed TICAM-1 (Figure 1B and 1C). These data suggested that the activation of RIG-I, IPS-1, or STING signaling, but not TICAM-1 signaling, induced p-TBK1 mitochondrial localization in HeLa cells.

Next, we examined the localization of p-TBK1 in HeLa cells after polyI:C or vertebrate dsDNA (salmon sperm DNA) stimulation. Previous studies reported that cytoplasmic vertebrate DNA induces Type I IFN expression [21,32]. When HeLa cells were stimulated with transfected polyI:C or dsDNA for 6 h, p-TBK1 levels increased (Figure 2A), and more than 80 % of p-TBK1 showed mitochondrial localization (Figure 2B and 2C). In contrast, when HeLa cells were stimulated with polyI:C without transfection to activate the TLR3 pathway, most of p-TBK1 did not localize on mitochondria (Figure 2B). These data indicated that p-TBK1 localized on mitochondria in response to cytoplasmic polyI:C or dsDNA but not to extracellular polyI:C.

Next, we compared the subcellular localization of p-TBK1 to other proteins after polyI:C transfection. We found that p-TBK1 colocalized with a mitochondrial protein MFN-1 (Figure 3A). In contrast, p-TBK1 barely colocalized with the stress granule marker G3BP (Figure 3A). To compare the p-TBK1 localization with IPS-1 and STING localizations, HA-tagged IPS-1 or FLAG-tagged STING were transfected into HeLa cells. At 24 h after transfection, cells were stimulated by mock or polyI:C transfection for 6 h. Although either IPS-1 or STING expression induced p-TBK1 staining without stimulation (Figure S1A and S1B), most p-TBK1 colocalized with HA-tagged IPS-1 but poorly colocalized with FLAG-tagged STING in both stimulated and mock-stimulated cells (Figure 3A and Figure S1). These data are consistent with previous observations that IPS-1, but not STING, is essential for Type I IFN production in response to polyI:C [6,25].

Next, we stimulated HeLa cells by dsDNA transfection. Interestingly, p-TBK1 colocalized with exogenously expressed HA-tagged IPS-1 (Figure 3B) in dsDNA stimulated HeLa cells, although IPS-1 is known to be dispensable for type I IFN production in response to DNA stimulation [33]. We found that p-TBK1 induced by DNA stimulation colocalized with a mitochondria marker MFN-1, and partially colocalized with a MAMs marker Presenilin-1 (PSEN-1) and exogenously expressed FLAG-tagged STING (Figure 3C-3E). Statistical analysis suggested that more than 60 % of p-TBK1 colocalized with HA-tagged IPS-1 and MFN-1, whereas less than 10 % of p-TBK1 colocalized with FLAG-tagged STING (Figure 3F). Approximately 30 % of p-TBK1 colocalized with PSEN-1 (Figure 3F). Taken together, these data suggested that most mitochondrial p-TBK1 induced by DNA transfection colocalized with IPS-1 and MFN-1 in HeLa cells. Because STING but not IPS-1 is essential for Type I IFN expression in response to cytoplasmic DNA [25,33], there appears to be an apparent contradiction between our subcellular localization and previous genetic data. Thus, we further focused on p-TBK1 localization induced by cytoplasmic DNA to dissect these apparently contradictory results.

Cell Type-Specific Localization of p-TBK1 in Response to Cytoplasmic DNA

We investigated whether p-TBK1 induced by DNA transfection exhibited mitochondrial localization in other cell lines. As seen with HeLa cells, in HepG2 cells, p-TBK1 exhibited mitochondrial localization in response to cytoplasmic DNA (Figure 4A and 4F). In contrast, most p-TBK1 did not exhibit mitochondrial localization in L929, RAW264.7, a mouse hepatocyte cell line [34], or tree shrew fibroblast T-23 cells [35] (Figure 4B-4E). Statistical analysis showed that fewer than 20% of p-TBK1 localized on mitochondria in the mouse hepatocyte cell line, L929, RAW264.7, and tree shrew T-23 cells (Figure 4F). Although p-TBK1 colocalized with exogenously expressed HA-tagged IPS-1 but not FLAG-tagged STING in dsDNA stimulated HeLa cells (Figure 3B and 3C), most p-TBK1 colocalized with exogenously expressed FLAG-tagged STING in dsDNA stimulated L929, RAW264.7, mouse hepatocytes or T-23 cells but not in HepG2 (Figure 5A-5F).

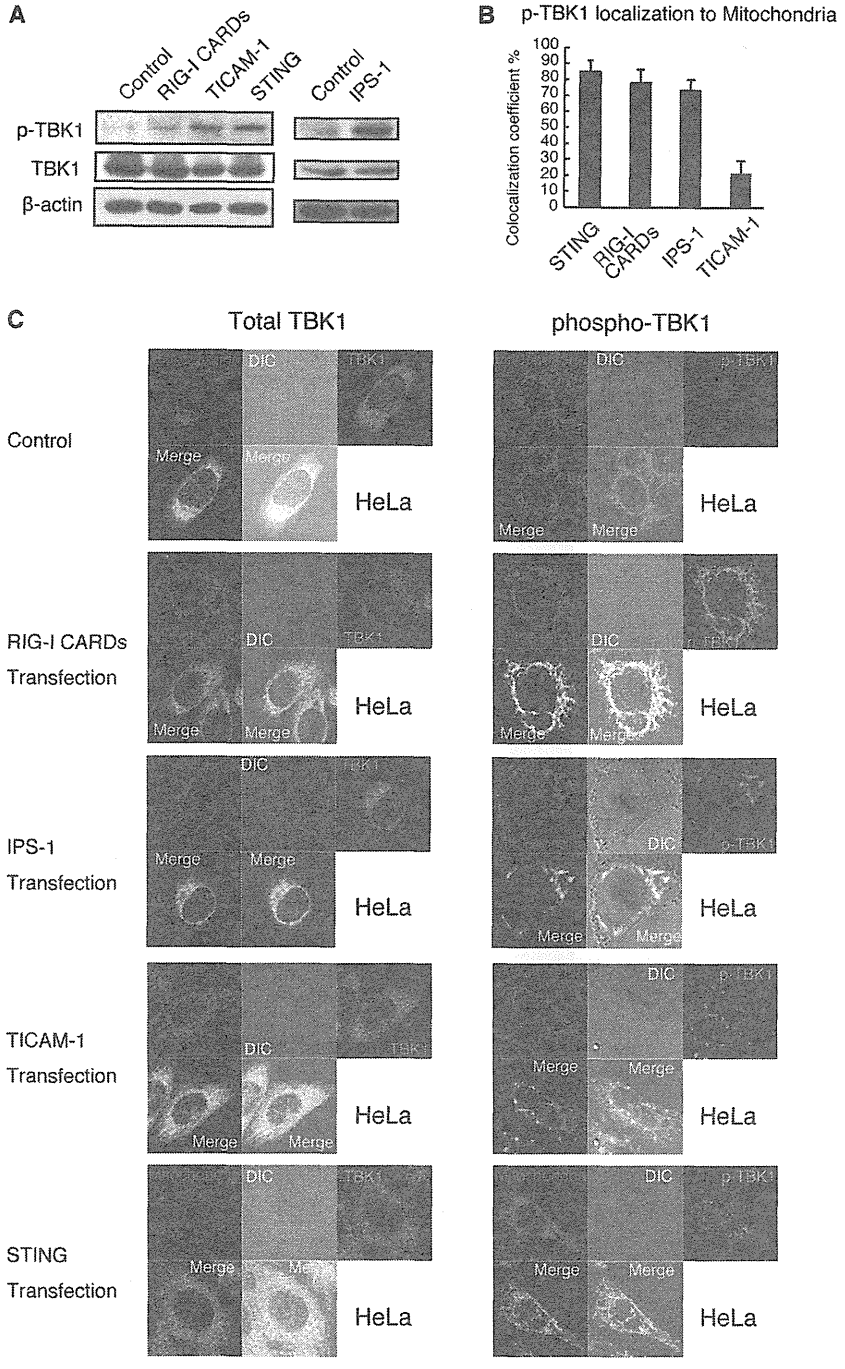

Figure 1. Mitochondrial localization of p-TBK1 in HeLa cells. (A) HeLa cells were transfected with 1.2 μg of empty vector, RIG-I CARDs, TICAM-1, IPS-1, or STING expression vectors in 6-well plate. At 24 h after transfection, cell lysates were prepared and subjected to SDS-PAGE. Proteins were detected by western blotting using anti-TBK1, p-TBK1, and β-actin antibodies.
(B and C) HeLa cells were transfected with 0.3 μg of empty vector or RIG-I CARDs, TICAM-1, or STING expression vectors in 24-well plate. At 24 h after transfection, cells were fixed and stained with anti-TBK1 or anti-p-TBK1 antibodies and Mitotracker Red. Colocalization coefficients of p-TBK1 with mitochondria were determined (mean ± sd, n = 3) (C). Unless otherwise indicated, Data are from one representative (n = 3) of at least three independent experiments.
doi: 10.1371/journal.pone.0083639.g001

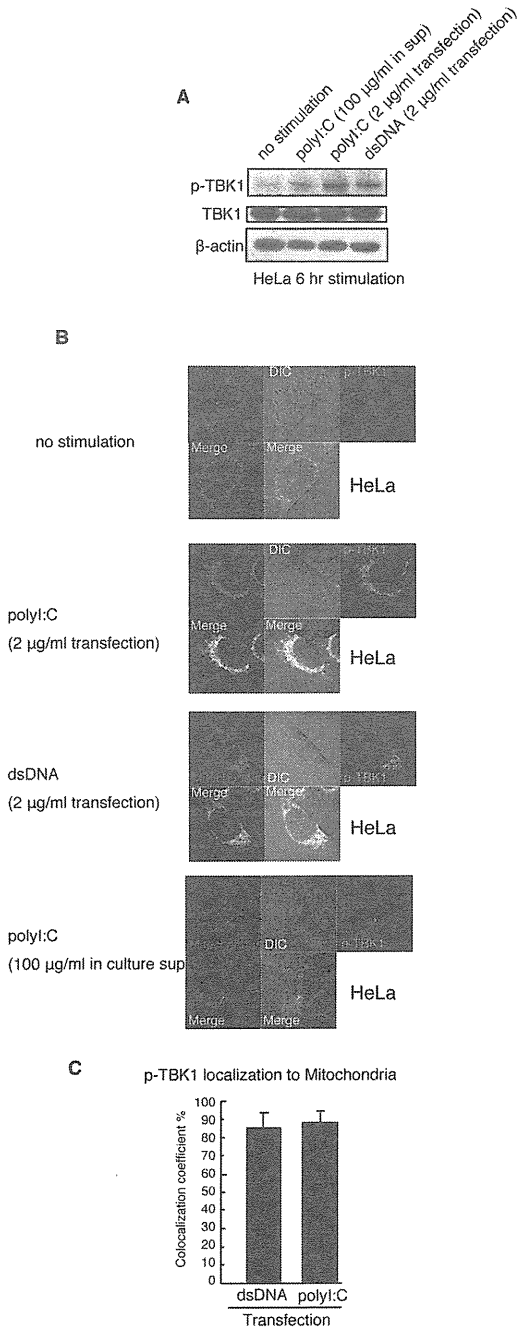

Figure 2. Mitochondrial localization of p-TBK1 in response to cytoplasmic nucleic acids in HeLa cells. (A) HeLa cells were stimulated with 100 μg/ml of polyI:C (no transfection), 2 μg/ml of polyI:C (by transfection) or 2 μg/ml of salmon sperm dsDNA (by transfection) in 6-well plate. At 6 h after stimulation, cell lysates were prepared and subjected to SDS-PAGE. Proteins were detected by western blotting using anti-TBK1, p-TBK1, and β-actin antibodies.

(B) HeLa cells were stimulated with 100 μg/ml of polyI:C (no transfection), 2 μg/ml of polyI:C (by transfection), or 2 μg/ml of salmon sperm dsDNA (by transfection) in 24-well plate. At 6 h after stimulation, cells were fixed and stained with anti p-TBK1 antibody and Mitotracker Red.

(C) Colocalization coefficients of p-TBK1 with mitochondria were determined (mean ±sd, n = 3).

doi: 10.1371/journal.pone.0083639.g002

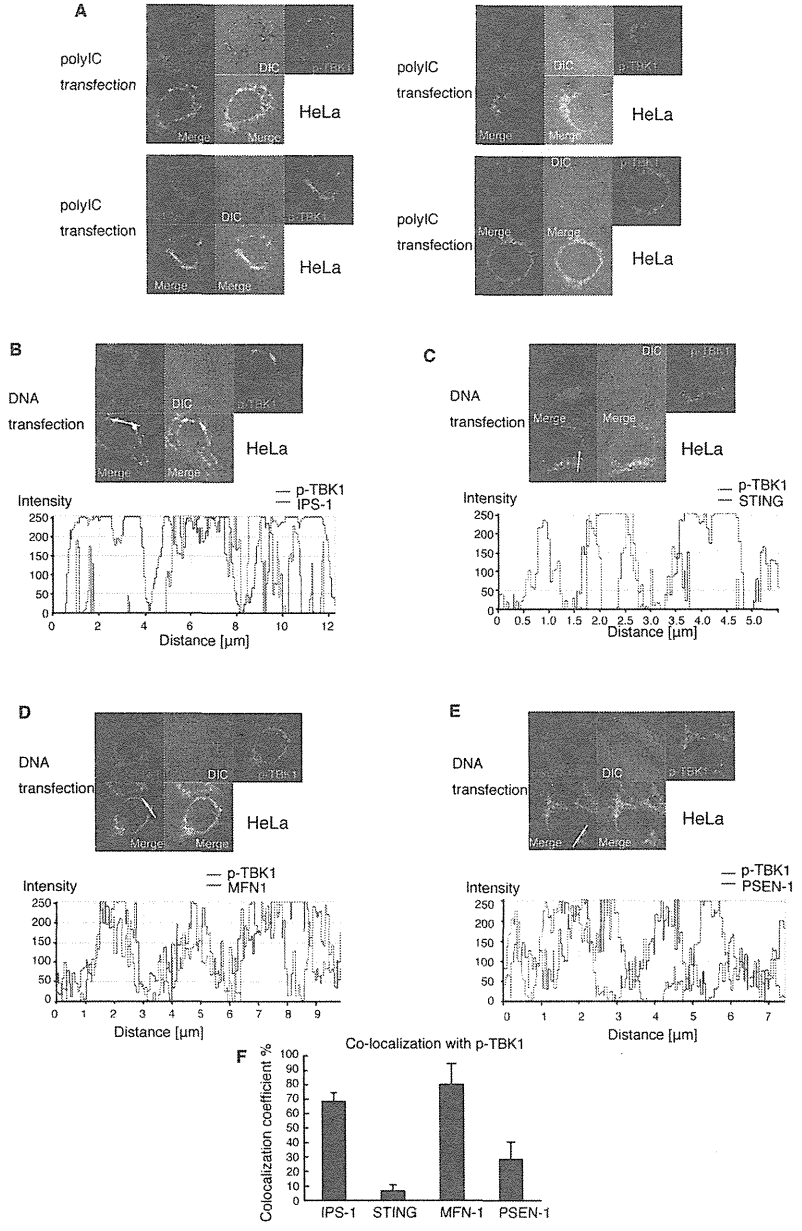

Figure 3. Co-localization of p-TBK1 with IPS-1 in HeLa cells. (A) HeLa cells were transfected with 1 μg of polyI:C in 24-well plate. At 6 h after transfection, cells were fixed and stained with anti-HA, p-TBK1, FLAG, MFN-1, and/or G3BP antibodies. To observe IPS-1 and STING localization, HeLa cells were transfected with HA-tagged IPS-1 or FLAG-tagged STING expression vectors 24 h before stimulation.

(B and C) HeLa cells were transfected with 0.3 μg of HA-tagged IPS-1 (B) or FLAG-tagged STING (C) expression vectors. At 24 h after transfection, HeLa cells were stimulated with 1 μg of salmon sperm dsDNA by transfection in 24-well plate. At 6 h after stimulation, cells were fixed and stained with anti-p-TBK1 and anti-HA or FLAG antibodies. Histograms display the measured fluorescence intensity along the white line in the merged panels.

(D and E) HeLa cells were stimulated with salmon sperm dsDNA by transfection. At 6 h after stimulation, cells were fixed and stained with anti-p-TBK1 and MFN-1 (D) or PSEN-1 antibodies (E). Histograms display the measured fluorescence intensity along the white line in the merged panels.

(F) Colocalization of coefficients of p-TBK1 with IPS-1, STING, MFN-1 or PSEN-1 are shown (mean ± sd, n = 3).

doi: 10.1371/journal.pone.0083639.g003

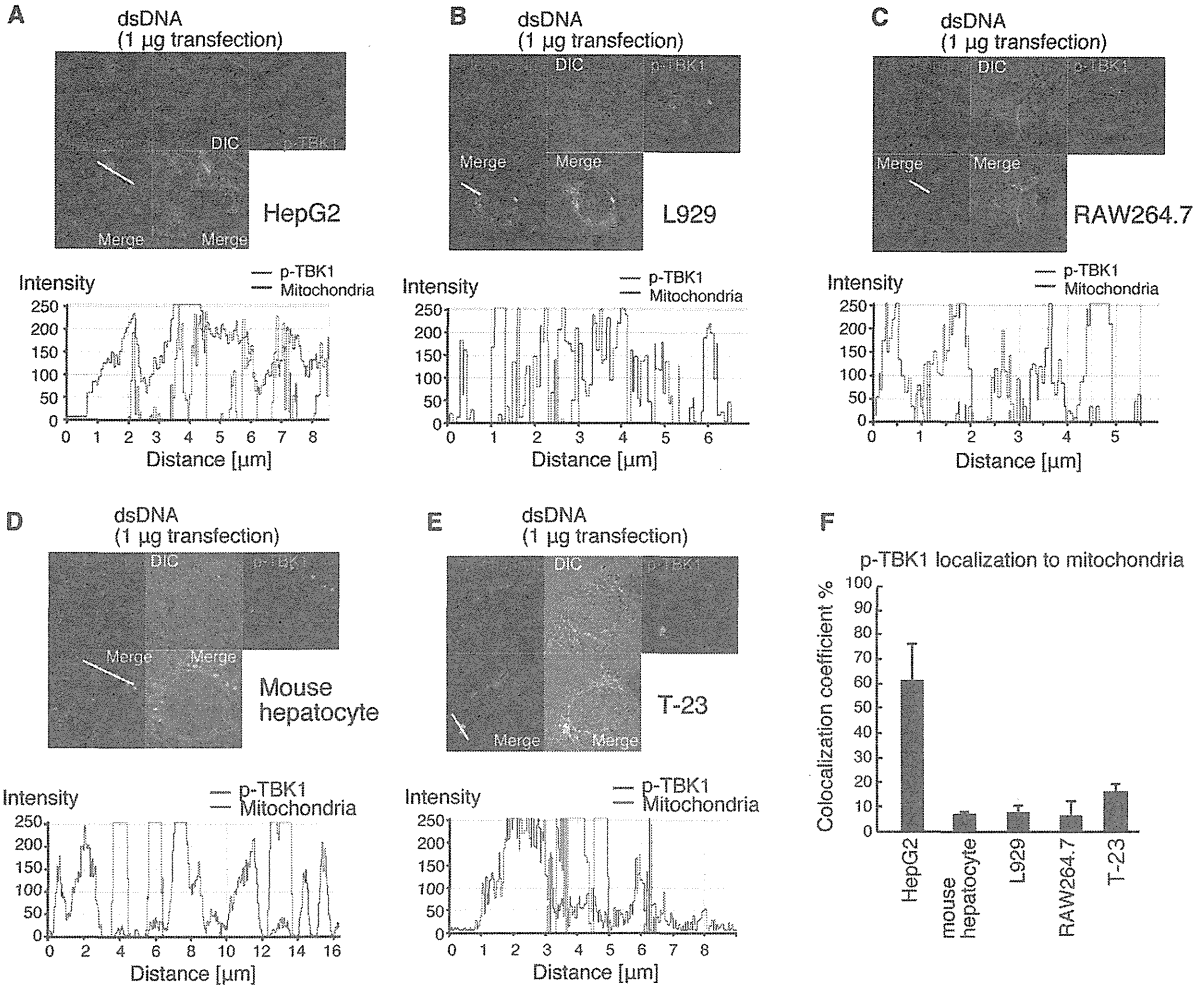

Figure 4. Cell type-specific localization of p-TBK1 in response to cytoplasmic dsDNA. (A-E) HepG2 (A), L929 (B), RAW264.7 (C), mouse hepatocyte (D), and T-23 (E) cells were stimulated with salmon sperm dsDNA by transfection. At 6 h after stimulation, cells were fixed and stained with anti-p-TBK1 antibody and Mitotracker Red. Histograms display the measured fluorescence intensity along the white line in the merged panels.
(F) Colocalization coefficients of p-TBK1 with mitochondria are shown (mean ± sd, n = 3).
doi: 10.1371/journal.pone.0083639.g004

These data suggested that p-TBK1 exhibited cell type-specific localization in response to cytoplasmic DNA.

p-TBK1 mitochondrial localization in response to cytoplasmic viral DNA in human cell lines

Next, we investigated p-TBK1 localization in response to viral DNA. Hepatitis B virus (HBV) is a DNA virus, and its protein HBx suppresses IFN-β mRNA expression in response to dsDNA but not to dsRNA [36], suggesting that DNA sensing pathway is targeted by HBV. When HBV full-length genomic DNA was transfected into HepG2, type I IFN mRNA expression was hardly induced (Figure S2). To avoid the suppression of innate immune response by HBV proteins transcribed from full-length HBV DNA, we used partial fragments of HBV genomic DNA (F1-F4) (Figure 6A). Stimulation with HBV genomic DNA fragments (F1-F4) efficiently induced *IFN-β* mRNA expression (Figure 6A and 6B). As observed with vertebrate DNA, the HBV genomic DNA fragment F1 induced mitochondrial localization of p-TBK1 (Figure 6C and 6D), and most p-TBK1 colocalized with IPS-1 but not STING in HepG2 cells (Figure 6C and 6D). When RAW264.7, the mouse hepatocyte cell line, or T-23 cells were stimulated with the HBV DNA fragment by transfection, p-TBK1 did not exhibit mitochondrial localization (Figure 7A, 7C,

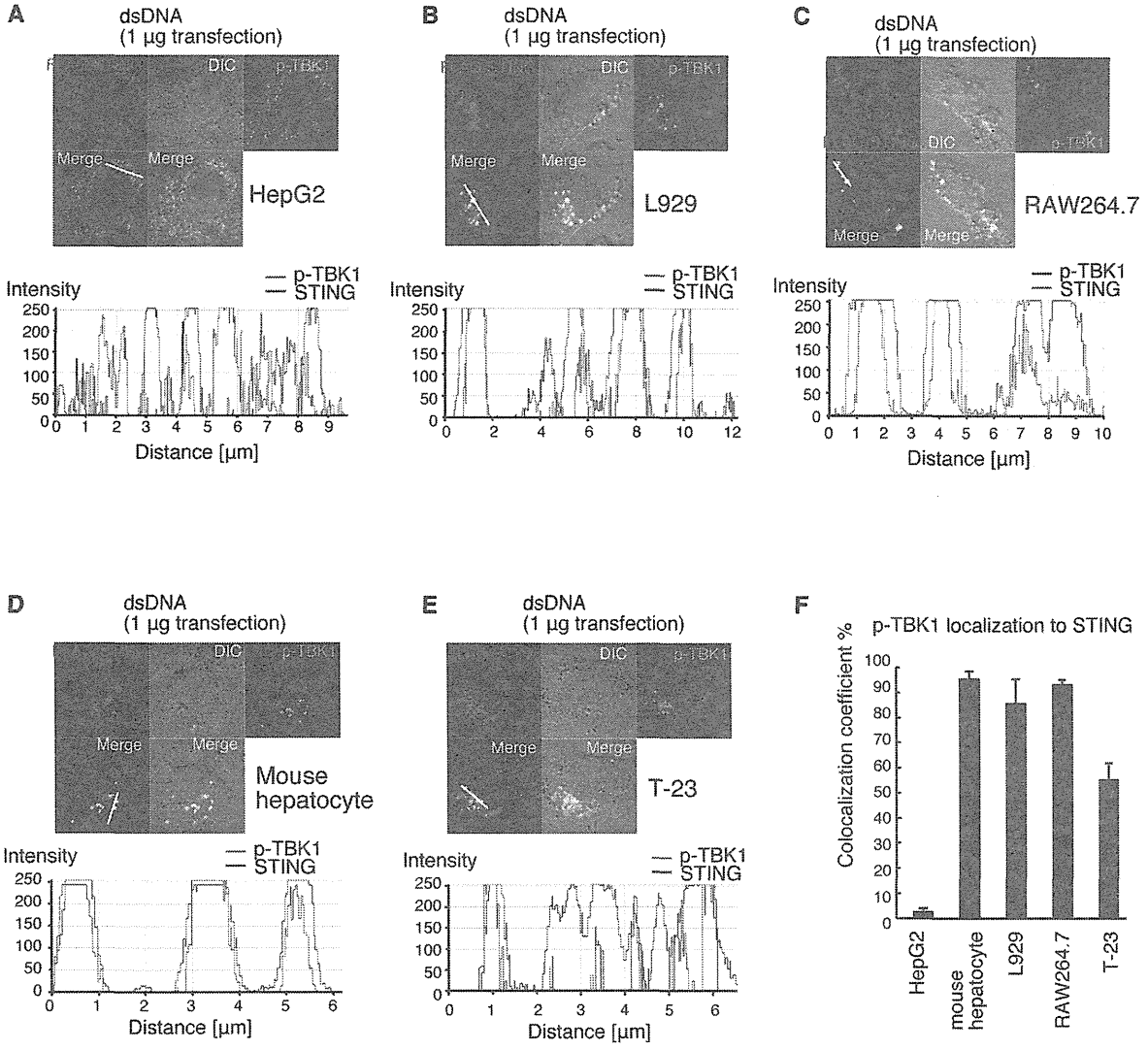

Figure 5. p-TBK1 colocalization with STING in mammalian cells in response to DNA. (A-E) 0.5 μg of FLAG-tagged STING expression vector was transfected into HepG2 (A), L929 (B), RAW264.7 (C), mouse hepatocytes (D) or T-23 (E) cells. At 24 h after transfection, cells were stimulated with salmon sperm dsDNA. At 6 h after transfection, cells were fixed and stained with anti-FLAG and p-TBK1 antibodies. Histograms display the measured fluorescence intensity along the white line in the merged panels.
(F) Colocalization coefficients of p-TBK1 with STING are shown (mean ± sd, n = 3).
doi: 10.1371/journal.pone.0083639.g005

and 7E), and more than 70% of p-TBK1 colocalized with STING (Figure 7B, 7D, and 7F).

Next, we investigated p-TBK1 localization after a DNA virus herpes simplex virus type-1 (HSV-1) infection in HeLa, HepG2, the mouse hepatocyte cell line, and T-23 cells. In HeLa and HepG2 cells, p-TBK1 localized on mitochondria, whereas, in the mouse hepatocyte cell line and T-23 cells, most p-TBK1 failed to localize on mitochondria (Figure 8A-8D). The statistic analysis indicated that the colocalization coefficient of p-TBK1 to mitochondria of HeLa or HepG2 cells was higher than that of mouse hepatocyte or T-23 cells (Figure 8E). Taken together, these data indicated that p-TBK1 exhibited mitochondrial localization in response to cytoplasmic viral DNA in HeLa and HepG2 cells, but not in RAW264.7, the mouse hepatocyte cell line, or T-23 cells.

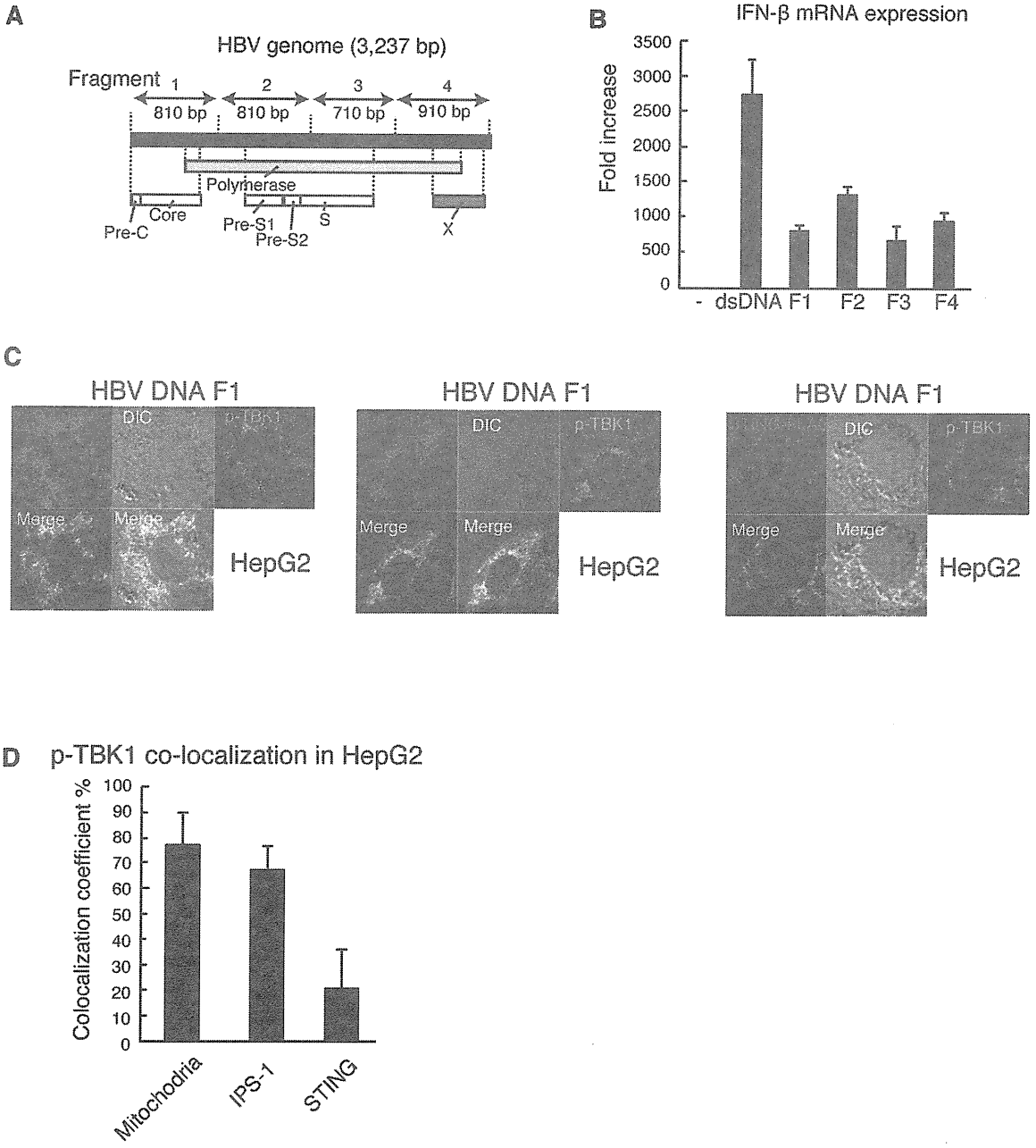

Figure 6. p-TBK1 colocalization with IPS-1 in response to a HBV genomic DNA fragment in HepG2 cells. (A) A schematic diagram of HBV genomic DNA fragments used in panels B-J.

(B) RAW264.7 cells were transfected with mock, salmon sperm dsDNA, or HBV dsDNA fragments F1, F2, F3, or F4. At 6 h after transfection, IFN-β mRNA expression was determined by RT-qPCR.

(C) HepG2 cells were transfected with 1 μg of HBV fragment 1 in 24-well plate. At 6 h after transfection, cells were fixed and stained with anti-p-TBK1 antibody and Mitotracker Red or anti-HA antibody. To observe IPS-1 and STING localization, 0.5 μg of HA-tagged IPS-1 or FLAG-tagged STING expression vector was transfected into HepG2 cells 24 h before stimulation.

(D) Colocalization coefficients of p-TBK1 with mitochondria, IPS-1, or STING (mean ± sd, n = 3).

doi: 10.1371/journal.pone.0083639.g006

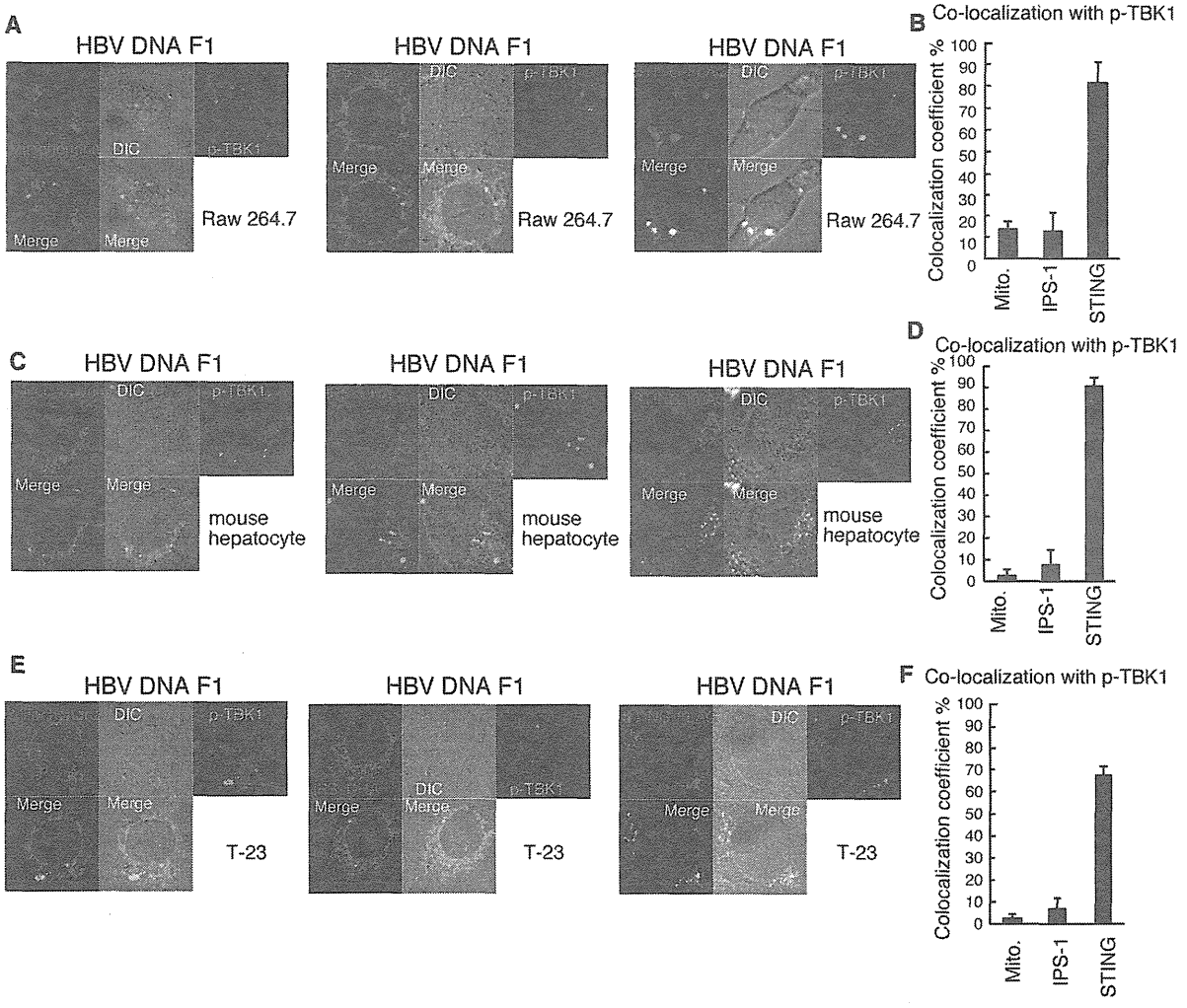

Figure 7. p-TBK1 colocalization with STING in response to a HBV genomic DNA fragment in mammalian cells. RAW264.7 (A and B), mouse hepatocyte (C and D), and T-23 (E and F) cells were transfected with HBV fragment 1. At 6 h after transfection, cells were fixed and stained with anti-p-TBK1 and FLAG antibodies and Mitotracker Red. To observe STING and IPS-1 localization, 0.5 μg of HA-tagged IPS-1 or FLAG-tagged STING expression vectors were transfected into RAW264.7 cells 24 h before stimulation. Colocalization coefficients of p-TBK1 with mitochondria (Mito.), IPS-1, or STING (mean ± sd, n = 3) in RAW264.7 (B), mouse hepatocyte (D), and T-23 (F) cells are shown.

doi: 10.1371/journal.pone.0083639.g007

IPS-1 is essential for TBK1 phosphorylation in HeLa cells in response to cytoplasmic DNA

As most p-TBK1 colocalized with IPS-1 in response to cytoplasmic DNA in HeLa cells, we investigated whether IPS-1 was required for TBK1 phosphorylation in response to cytoplasmic DNA in HeLa cells. We transfected siRNA for negative control or *IPS-1* into HeLa cells. At 48 h after transfection, cells were stimulated with the HBV DNA fragment F1 or salmon sperm dsDNA by transfection. We confirmed that siRNA for *IPS-1* markedly reduced *IPS-1* mRNA levels in both mock and dsDNA stimulated cells (Figure S3). Interestingly, siRNA for *IPS-1* reduced p-TBK1 staining in HeLa cells (Figure 9A). As STING is essential for Type I IFN expression in response to cytoplasmic DNA, we investigated the requirement for STING in TBK1 phosphorylation in response to HBV DNA. Our results showed that siRNA for *STING* reduced STING mRNA levels and abrogated p-TBK1 staining (Figure 9A and Figure S3). Next, we investigated p-TBK1 levels in cell lysates by western blotting and found that knockdown of *IPS-1* reduced p-TBK1 levels induced by DNA stimulation (Figure 9B). siRNA for *STING* also reduced p-TBK1 levels (Figure 9C)

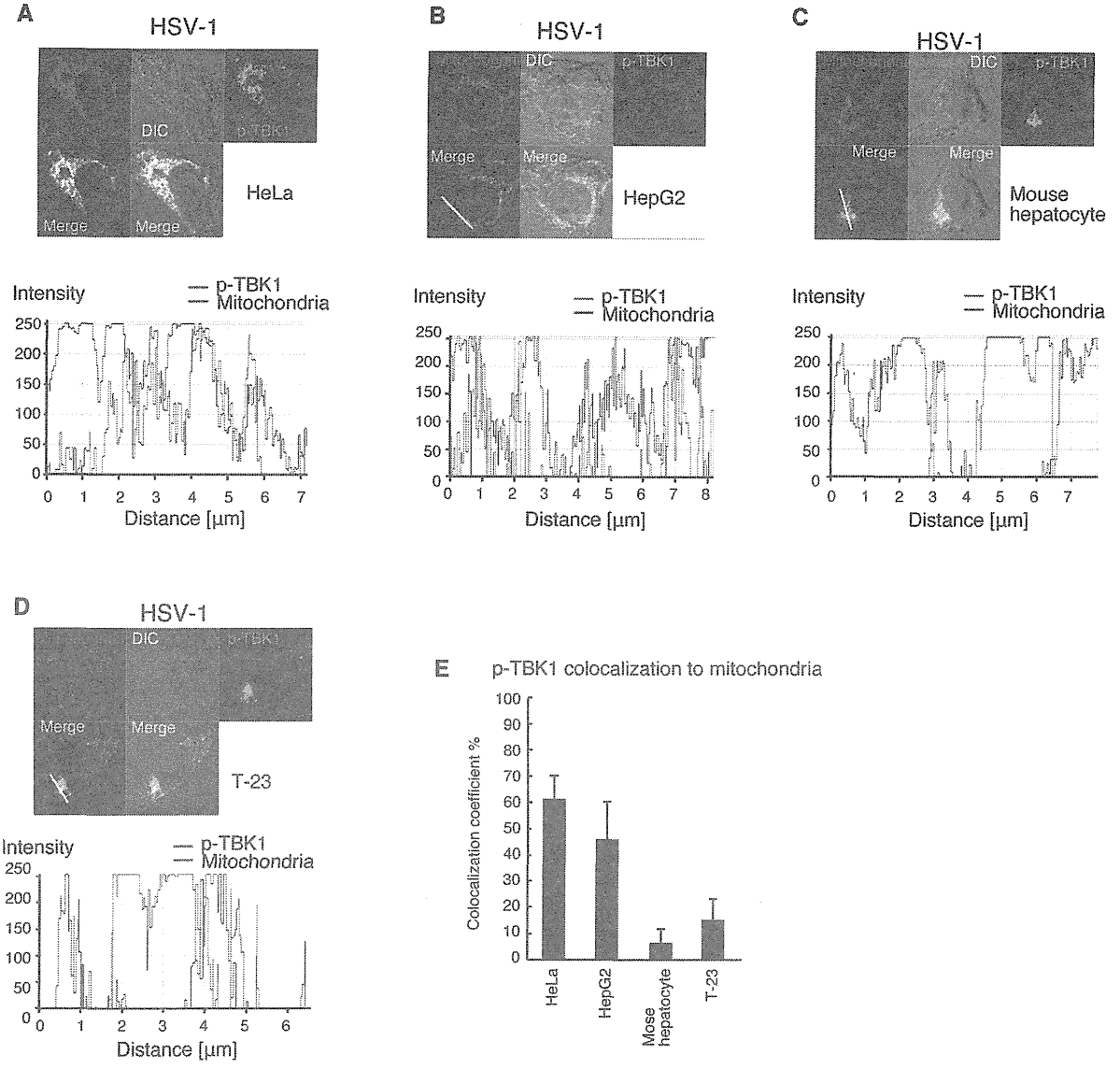

Figure 8. p-TBK1 localization in response to HSV-1 infection. HeLa (A), HepG2 (B), mouse hepatocyte (C), and T-23 (D) cells were infected with HSV-1 for 24 h. Cells were fixed and stained with Mitotracker Red and anti-p-TBK1 antibody. Histograms display the measured fluorescence intensity along the white line in the merged panels. Colocalization coefficients of p-TBK1 to mitochondria are shown (E).

doi: 10.1371/journal.pone.0083639.g008

Next, we investigated whether siRNA for *IPS-1* or *STING* reduces IFN-β mRNA expression in response to DNA stimulation. siRNA for *IPS-1* significantly reduced IFN-β mRNA expression in response to vertebrate DNA and HBV DNA F1 fragment in HeLa cells (Figure 9D), whereas siRNA for *IPS-1* failed to reduce IFN-β mRNA expression in response to vertebrate DNA in L929 cells (Figure S3B). siRNA for *STING* also reduced IFN-β mRNA expression in HeLa cells (Figure 9D). Taken together, these data indicated that IPS-1, as well as STING, are required for TBK1 phosphorylation and efficient IFN-β mRNA expression in response to cytoplasmic DNA in HeLa cells.

Next, we compared dsDNA-induced type I IFN mRNA expressions among human and mouse cells. HeLa cells were less responsive to DNA stimulation compared to THP-1, L929, and RAW264.7 cells (Figure 10A). Therefore, there is a

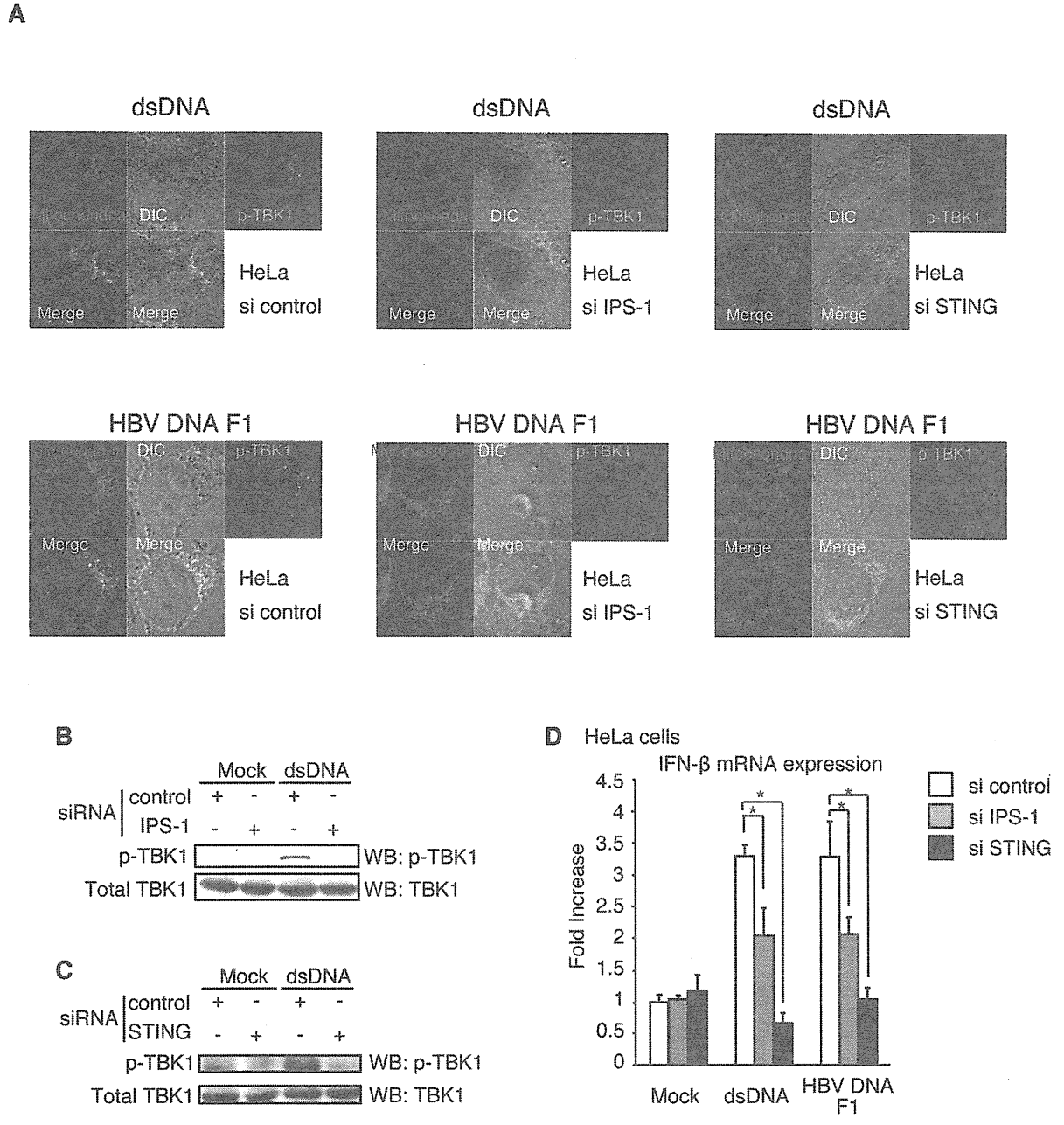

Figure 9. p-TBK1 levels in IPS-1 or STING knockdown cells. (A-C) siRNA for negative control, IPS-1, or STING were transfected into HeLa cells. At 48 h after transfection, cells were stimulated with HBV F1 fragment or salmon sperm DNA for 6 h. Cells were fixed and stained with Mitotracker Red and anti-p-TBK1 antibody (A), or cell lysates were prepared and subjected to SDS-PAGE and western blotting (B and C).

(D) siRNA for IPS-1 or STING were transfected into HeLa cells At 48 h after transfection, cells were stimulated with mock, HBV F1 fragment, or salmon sperm DNA (dsDNA) for 6 h. The IFN-β mRNA expression was determined by RT-qPCR.

doi: 10.1371/journal.pone.0083639.g009

possibility that mitochondrial localization might correlate with a lack of strong response of the cells to the cytoplasmic DNA stimulation. To test this possibility, we investigated p-TBK1 subcellular localization in THP-1, which efficiently expressed IFN-β mRNA in response to DNA stimulation as L929 cells (Figure 10A). p-TBK1 showed mitochondrial localization in response to salmon sperm DNA or HBV F1 DNA fragment in THP-1 cells (Figure 10B). This observation weakened the possibility.

Discussion

Autophosphorylation of TBK1 is essential for Type I IFN expression [28]. Here, we demonstrated that p-TBK1 is localized on mitochondria in response to cytoplasmic DNA in HeLa and HepG2 cells. p-TBK1 induced by DNA stimulation in HeLa and HepG2 cells co-localized with IPS-1 and MFN-1. Moreover, knockdown of *IPS-1* reduced p-TBK1 levels in response to viral DNA in HeLa cells. These data indicate that IPS-1 plays a crucial role in the phosphorylation of TBK1 in response to cytoplasmic DNA in the human cells. In contrast, p-TBK1 did not localize on mitochondria in the mouse or tree shrew cells that we tested. This is consistent with a previous knockout mouse study that showed that IPS-1 is dispensable for the response to cytoplasmic DNA [33]. Thus, there appears to be species-specific mechanisms of Type I IFN production in response to cytoplasmic DNA. However, we do not exclude the possibility that some of human primary or immortalized cells do not exhibit IPS-1 mitochondrial localization in response to cytoplasmic viral DNA. Taniguchi and colleagues firstly reported cell type-specific roles of a DNA sensor, DAI, in a cytoplasmic DNA sensing pathway [32,37]. Later, other groups reported several other DNA sensors using various types of cells [38]. Recently Chen and colleagues showed that cGAS is essential for type I IFN production in response to poly(dA:dT) in plasmacytoid DC but not in lung fibroblasts [39]. Their findings suggested that RNA polymerase III – RIG-I pathway plays a major role in sensing DNA in lung fibroblasts [24]. Thus, these observations indicate that there are several cell type-specific DNA sensing pathways. Our observations of cell type-specific p-TBK1 localization in response to cytoplasmic DNA also support this model.

Gale and colleagues previously reported that a major site of IPS-1 signaling is MAMs [8]. TBK1 autophosphorylation in response to HBV DNA required both IPS-1 and STING in human cells that we tested. Considering that IPS-1 and STING localize on the mitochondria and ER, respectively, it is expected that TBK1 autophosphorylation occurs within MAMs where the ER associates with mitochondria in response to cytoplasmic viral DNA in HeLa and HepG2 cells. Indeed, a fraction of cellular p-TBK1 was localized on MAMs. It is likely that TBK1 moved to mitochondria after autophosphorylation in human cells. In contrast, mouse and tree shrew TBK1 appears to be phosphorylated on ER where STING localizes. The biological significance of the mitochondrial or ER localization of p-TBK1 is unclear. A previous report demonstrated that peroxisomal IPS-1 triggers rapid expression of ISGs, whereas mitochondrial IPS-1 triggers delayed ISG and IFN expression

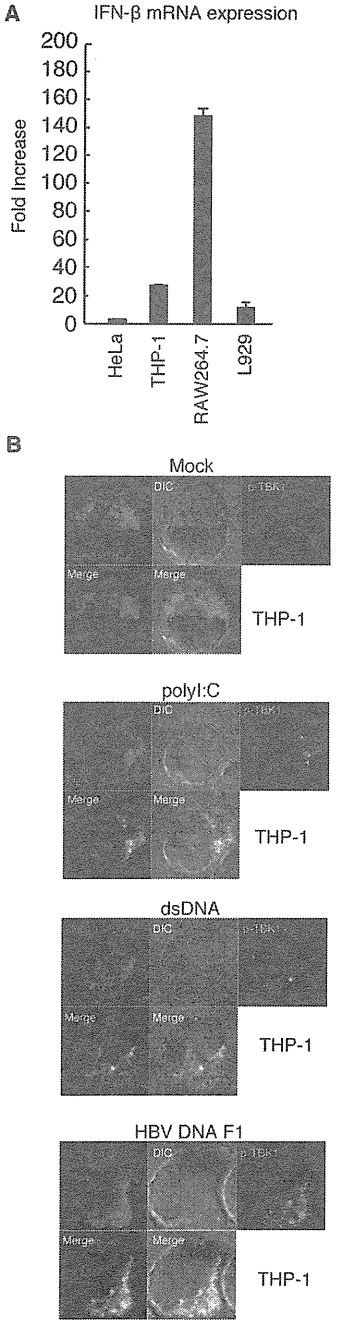

Figure 10. Subcellular localization of p-TBK1 in response to polyI:C or DNA in THP-1 cells. (A) HeLa, THP-1, Raw264.7, and L929 cells were stimulate with salmon sperm DNA for 6 h by transfection. The fold increase of IFN-β mRNA expression in response to DNA was determined by RT-qPCR. (B) THP-1 cells were stimulated with mock, polyI:C, salmon sperm DNA (dsDNA), or HBV DNA F1 for 3 h. Cells were fixed and stained with Mitotracker Red and anti-p-TBK1 antibody.

doi: 10.1371/journal.pone.0083639.g010

[7]. Thus, as observed with IPS-1, differential p-TBK1 placement may allow the cell to diversify signaling pathways.

When human STING or IPS-1 were transfected into mouse cells, p-TBK1 did not localize on the mitochondria in response to cytoplasmic DNA. Thus, the differences in the STING and IPS-1 protein sequences between humans and mice are not a cause of the cell type-specific localization of p-TBK1. It is possible that the difference in TBK1 protein sequence between humans and mice determines the cell type specific localization of p-TBK1. Another possibility is that an unknown factor of human or mouse associate with TBK1 or p-TBK1. Our current knowledge cannot explain the cell type-specific localization of p-TBK1 in response to cytoplasmic DNA stimulation. Further study is required to reveal the precise mechanisms used by cytoplasmic DNA sensing pathways.

Materials and Methods

Cells, viruses, and reagents

A tree shrew (*Tupaia belangeri*) fibroblast cell line, T-23 (clone 8) cells were obtained from JCRB. T-23 and HepG2 cells were cultured in Dulbecco's modified Eagle's medium low glucose medium (D-MEM) with 10% heat-inactivated fetal calf serum (FCS) (Invitrogen). HeLa cells were cultured in minimum Eagle's medium with 2 mM L-glutamine and 10% heat-inactivated FCS. Protocols for the isolation and culture conditions of mouse hepatocytes have been described previously [34]. L929 and RAW264.7 cells were cultured in RPMI1640 with 10% of FCS. Salmon sperm DNA and polyI:C were purchased from Invitrogen or GE Healthcare, respectively. HSV-1 K strain was amplified using Vero cells. To determine viral titers, we performed plaque assay using Vero cells. Vero cells were cultured in D-MEM with 10% of FCS. THP-1 cells were cultured in RPMI1640 with 10 % FCS and 0.1 % 2-mercaptoethanol.

Confocal Microscopy

Phospho-TBK1/NAK (Ser 172) (D52C2) XP rabbit mAb were purchased from Cell Signaling. Anti-Presenilin 1 Ab [APS11], anti-NAK (TBK1) Ab (EP611Y), anti-mitofusin 1 Ab, and anti-G3BP Ab were purchased from Abcam. Anti-FLAG antibody was purchased from Sigma-Aldrich. Anti-HA Ab [HA1.1] was purchased from COVANCE. Mitotracker Red was purchased from Life Technologies. Cells were fixed with 3% of formaldehyde in 1x PBS for 30 min, and permeabilized with 0.2% Triton X-100 in 1 x PBS for 15 min. In case of PSEN-1 staining, fixed cells were permeabilized with 0.5% of saponin in 1x PBS with 1 % BSA for 30 min. For blocking, 1% BSA in PBS was used for 30 min. The cells were labeled with the indicated primary antibody for 60 min at room temperature. After washing four times with 1% BSA in PBS, cells were incubated with an Alexa-conjugated secondary antibody and 1% BSA in PBS for 30 min at room temperature, and then were washed four times with 1% BSA in PBS. Samples were mounted on glass slides using Prolong Gold (Invitrogen). Cells were visualized at a magnification of ×63 with an LSM510 META microscope (Zeiss). Colocalization of coefficients and intensity histograms were determined using LSM510 ZEISS LSM Image examiner software.

Plasmids

RIG-I CARDs expression vector (dRIG-I) has been described previously [40]. Human *IPS-1* cDNA encoding the full-length ORF was cloned into a pEF-BOS multi-cloning site, and an HA sequence was inserted just before the STOP codon. Human *STING* cDNA that encoded a full-length ORF was cloned into a pEF-BOS multi-cloning site, and a FLAG-tag sequence was inserted just before the STOP codon. The plasmids were sequenced to confirm that there were no PCR errors.

HBV DNA preparation and quantitative PCR

HBV DNA fragments were obtained by PCR using HBV DNA as a template. A plasmid carrying HBV full-length genomic DNA were kindly gifted from Chayama K. Primer sequences were as follows: F1 forward, TGC AAC TTT TTC ACC TCT GC; F1 reverse, TCT CCT TTT TTC ATT AAC TG; F2 forward, TTA AAA TTA ATT ATG CCT GC; F2 reverse, AAC AAG AAA AAC CCC GCC TG; F3 forward, GAC AAG AAT CCT CAC AAT AC; F3 reverse, TGT ACA ATA TGT TCT TGT GG; F4 forward, AAA AAT CAA GCA ATG TTT TC; and F4 reverse, ATT AGG CAG AGG TGA AAA AG. Amplified DNA fragments were purified using a Gel Extraction kit (Qiagen). For quantitative PCR (qPCR), total RNA was extracted using TRIZOL reagent (Invitrogen), after which 0.1-1 μg of RNA was reverse-transcribed using a high capacity cDNA transcription kit with an RNase inhibitor kit (Applied Biosystems) according to the manufacturer's instructions. qPCR was performed using a Step 1 real time PCR system (Applied Biosystems). The expression of cytokines mRNA was normalized to that of *GAPDH* or *β-actin* mRNA, and the fold-increase was determined by dividing the expressions in each sample by that of the wild-type at 0 h. The primers used for qPCR were described previously [40,41].

Supporting Information

Figure S1. HeLa cells were transfected with HA-tagged IPS-1 (A) or FLAG-tagged STING (B). At 24 h after transfection, cells were mock-stimulated for 6 h, and then fixed and stained with anti-p-TBK1 and HA or FLAG Abs.
(TIF)

Figure S2. HepG2 cells were transfected with a vector carrying 1.4 x HBV genomic DNA. Total RNA was extracted at indicated hours. IFN-β mRNA expression was determined by RT-qPCR.
(TIF)

Figure S3. siRNAs for control, IPS-1, or STING were transfected into HeLa and L929 cells. 48 h after transfection, cells were stimulated with or without dsDNA for 6 h. Total RNA was extracted with TRIZOL, and RT-qPCR was performed. IPS-1 and STING mRNA expressions were normalized with β-actin mRNA expression. Relative ratio was calculated by

dividing each ratio by the ratio of the "mock si control" sample. The target sequences of siRNA for human *IPS-1* and *STING* are: CCA AAG UGC CUA CCA CCU U and GGA UUC GAA CUU ACA AUC A, respectively. The target sequence of siRNA for mouse *IPS-1* and *STING* are: UGU UGC CUC UGU UCC CAUA and GCA CAU UCG UCA GGA AGA A, respectively. Silencer Select siRNAs were purchased from Life Technologies.
(TIF)

Acknowledgements

Plasmids carrying HBV genomic DNA were kindly gifted from Chayama K (Hiroshima University, Japan) and Chisari FV (The Scripps Research Institute, USA).

Author Contributions

Conceived and designed the experiments: HO M. Matsumoto T. Seya. Performed the experiments: T. Suzuki HO M. Miyashita. Analyzed the data: T. Suzuki HO M. Miyashita. Contributed reagents/materials/analysis tools: HA. Wrote the manuscript: HO T. Seya.

References

1. Loo YM, Gale M Jr. (2011) Immune signaling by RIG-I-like receptors. Immunity 34: 680-692. doi:10.1016/j.immuni.2011.05.003. PubMed: 21616437.
2. Onomoto K, Jogi M, Yoo JS, Narita R, Morimoto S et al. (2012) Critical role of an antiviral stress granule containing RIG-I and PKR in viral detection and innate immunity. PLOS ONE 7: e43031. doi:10.1371/journal.pone.0043031. PubMed: 22912779.
3. Xu LG, Wang YY, Han KJ, Li LY, Zhai Z et al. (2005) VISA is an adapter protein required for virus-triggered IFN-beta signaling. Mol Cell 19: 727-740. doi:10.1016/j.molcel.2005.08.014. PubMed: 16153868.
4. Seth RB, Sun L, Ea CK, Chen ZJ (2005) Identification and characterization of MAVS, a mitochondrial antiviral signaling protein that activates NF-kappaB and IRF 3. Cell 122: 669-682. doi:10.1016/j.cell.2005.08.012. PubMed: 16125763.
5. Meylan E, Curran J, Hofmann K, Moradpour D, Binder M et al. (2005) Cardif is an adaptor protein in the RIG-I antiviral pathway and is targeted by hepatitis C virus. Nature 437: 1167-1172. doi:10.1038/nature04193. PubMed: 16177806.
6. Kawai T, Takahashi K, Sato S, Coban C, Kumar H et al. (2005) IPS-1, an adaptor triggering RIG-I- and Mda5-mediated type I interferon induction. Nat Immunol 6: 981-988. doi:10.1038/ni1243. PubMed: 16127453.
7. Dixit E, Boulant S, Zhang Y, Lee AS, Odendall C et al. (2010) Peroxisomes are signaling platforms for antiviral innate immunity. Cell 141: 668-681. doi:10.1016/j.cell.2010.04.018. PubMed: 20451243.
8. Horner SM, Liu HM, Park HS, Briley J, Gale M Jr. (2011) Mitochondrial-associated endoplasmic reticulum membranes (MAM) form innate immune synapses and are targeted by hepatitis C virus. Proc Natl Acad Sci U S A 108: 14590-14595. doi:10.1073/pnas.1110133108. PubMed: 21844353.
9. Onoguchi K, Onomoto K, Takamatsu S, Jogi M, Takemura A et al. (2010) Virus-infection or 5'ppp-RNA activates antiviral signal through redistribution of IPS-1 mediated by MFN1. PLoS Pathog 6: e1001012. PubMed: 20661427.
10. Yasukawa K, Oshiumi H, Takeda M, Ishihara N, Yanagi Y et al. (2009) Mitofusin 2 inhibits mitochondrial antiviral signaling. Sci Signal 2: ra47. PubMed: 19690333.
11. Hou F, Sun L, Zheng H, Skaug B, Jiang QX et al. (2011) MAVS forms functional prion-like aggregates to activate and propagate antiviral innate immune response. Cell 146: 448-461. doi:10.1016/j.cell.2011.06.041. PubMed: 21782231.
12. Perry AK, Chow EK, Goodnough JB, Yeh WC, Cheng G (2004) Differential requirement for TANK-binding kinase-1 in type I interferon responses to toll-like receptor activation and viral infection. J Exp Med 199: 1651-1658. doi:10.1084/jem.20040528. PubMed: 15210743.
13. Hemmi H, Takeuchi O, Sato S, Yamamoto M, Kaisho T et al. (2004) The roles of two IkappaB kinase-related kinases in lipopolysaccharide and double stranded RNA signaling and viral infection. J Exp Med 199: 1641-1650. doi:10.1084/jem.20040520. PubMed: 15210742.
14. Oshiumi H, Matsumoto M, Funami K, Akazawa T, Seya T (2003) TICAM-1, an adaptor molecule that participates in Toll-like receptor 3-mediated interferon-beta induction. Nat Immunol 4: 161-167. doi:10.1038/ni886. PubMed: 12539043.
15. Matsumoto M, Funami K, Tanabe M, Oshiumi H, Shingai M et al. (2003) Subcellular localization of Toll-like receptor 3 in human dendritic cells. J Immunol 171: 3154-3162. PubMed: 12960343.
16. Alexopoulou L, Holt AC, Medzhitov R, Flavell RA (2001) Recognition of double-stranded RNA and activation of NF-kappaB by Toll-like receptor 3. Nature 413: 732-738. doi:10.1038/35099560. PubMed: 11607032.
17. Sun L, Wu J, Du F, Chen X, Chen ZJ (2013) Cyclic GMP-AMP synthase is a cytosolic DNA sensor that activates the type I interferon pathway. Science 339: 786-791. doi:10.1126/science.1232458. PubMed: 23258413.
18. Kondo T, Kobayashi J, Saitoh T, Maruyama K, Ishii KJ et al. (2013) DNA damage sensor MRE11 recognizes cytosolic double-stranded DNA and induces type I interferon by regulating STING trafficking. Proc Natl Acad Sci U S A 110: 2969-2974. doi:10.1073/pnas.1222694110. PubMed: 23388631.
19. Desmet CJ, Ishii KJ (2012) Nucleic acid sensing at the interface between innate and adaptive immunity in vaccination. Nat Rev Immunol 12: 479-491. doi:10.1038/nri3247. PubMed: 22728526.
20. Stetson DB, Medzhitov R (2006) Recognition of cytosolic DNA activates an IRF3-dependent innate immune response. Immunity 24: 93-103. doi:10.1016/j.immuni.2005.12.003. PubMed: 16413926.
21. Ishii KJ, Coban C, Kato H, Takahashi K, Torii Y et al. (2006) A Toll-like receptor-independent antiviral response induced by double-stranded B-form. DNA - Nat Immunol 7: 40-48. doi:10.1038/ni1282.
22. Choi MK, Wang Z, Ban T, Yanai H, Lu Y et al. (2009) A selective contribution of the RIG-I-like receptor pathway to type I interferon responses activated by cytosolic. DNA - Proc Natl Acad Sci U S A 106: 17870-17875. doi:10.1073/pnas.0909545106.
23. Cheng G, Zhong J, Chung J, Chisari FV (2007) Double-stranded DNA and double-stranded RNA induce a common antiviral signaling pathway in human cells. Proc Natl Acad Sci U S A 104: 9035-9040. doi:10.1073/pnas.0703285104. PubMed: 17517627.
24. Chiu YH, Macmillan JB, Chen ZJ (2009) RNA polymerase III detects cytosolic DNA and induces type I interferons through the RIG-I pathway. Cell 138: 576-591. doi:10.1016/j.cell.2009.06.015. PubMed: 19631370.
25. Ishikawa H, Ma Z, Barber GN (2009) STING regulates intracellular DNA-mediated, type I interferon-dependent innate immunity. Nature 461: 788-792. doi:10.1038/nature08476. PubMed: 19776740.
26. Ishikawa H, Barber GN (2008) STING is an endoplasmic reticulum adaptor that facilitates innate immune signalling. Nature 455: 674-678. doi:10.1038/nature07317. PubMed: 18724357.
27. Ishii KJ, Kawagoe T, Koyama S, Matsui K, Kumar H et al. (2008) TANK-binding kinase-1 delineates innate and adaptive immune responses to DNA vaccines. Nature 451: 725-729. doi:10.1038/nature06537. PubMed: 18256672.
28. Soulat D, Bürckstümmer T, Westermayer S, Goncalves A, Bauch A et al. (2008) The DEAD-box helicase DDX3X is a critical component of the TANK-binding kinase 1-dependent innate immune response. EMBO J 27: 2135-2146. doi:10.1038/emboj.2008.126. PubMed: 18583960.
29. Fitzgerald KA, McWhirter SM, Faia KL, Rowe DC, Latz E et al. (2003) IKKepsilon and TBK1 are essential components of the IRF3 signaling pathway. Nat Immunol 4: 491-496. doi:10.1038/ni921. PubMed: 12692549.

30. Oshiumi H, Miyashita M, Matsumoto M, Seya T (2013) A Distinct Role of Riplet-Mediated K63-Linked Polyubiquitination of the RIG-I Repressor Domain in Human Antiviral Innate Immune Responses. PLOS Pathog 9: e1003533.
31. Yoneyama M, Kikuchi M, Natsukawa T, Shinobu N, Imaizumi T et al. (2004) The RNA helicase RIG-I has an essential function in double-stranded RNA-induced innate antiviral responses. Nat Immunol 5: 730-737. doi:10.1038/ni1087. PubMed: 15208624.
32. Takaoka A, Wang Z, Choi MK, Yanai H, Negishi H et al. (2007) DAI (DLM-1/ZBP1) is a cytosolic DNA sensor and an activator of innate immune response. Nature 448: 501-505. doi:10.1038/nature06013. PubMed: 17618271.
33. Kumar H, Kawai T, Kato H, Sato S, Takahashi K et al. (2006) Essential role of IPS-1 in innate immune responses against RNA viruses. J Exp Med 203: 1795-1803. doi:10.1084/jem.20060792. PubMed: 16785313.
34. Aly HH, Oshiumi H, Shime H, Matsumoto M, Wakita T et al. (2011) Development of mouse hepatocyte lines permissive for hepatitis C virus (HCV). PLOS ONE 6: e21284. doi:10.1371/journal.pone.0021284. PubMed: 21731692.
35. Taketomi M, Nishi Y, Ohkawa Y, Inui N (1986) Establishment of lung fibroblastic cell lines from a non-human primate Tupaia belangeri and their use in a forward gene mutation assay at the hypoxanthine-guanine phosphoribosyl transferase locus. Mutagenesis 1: 359-365. doi:10.1093/mutage/1.5.359. PubMed: 3331674.
36. Kumar M, Jung SY, Hodgson AJ, Madden CR, Qin J et al. (2011) Hepatitis B virus regulatory HBx protein binds to adaptor protein IPS-1 and inhibits the activation of beta interferon. J Virol 85: 987-995. doi: 10.1128/JVI.01825-10. PubMed: 21068253.
37. Wang Z, Choi MK, Ban T, Yanai H, Negishi H et al. (2008) Regulation of innate immune responses by DAI (DLM-1/ZBP1) and other DNA-sensing molecules. Proc Natl Acad Sci U S A 105: 5477-5482. doi: 10.1073/pnas.0801295105. PubMed: 18375758.
38. Paludan SR, Bowie AG (2013) Immune sensing of DNA. Immunity 38: 870-880. doi:10.1016/j.immuni.2013.05.004. PubMed: 23706668.
39. Li XD, Wu J, Gao D, Wang H, Sun L et al. (2013) Pivotal roles of cGAS-cGAMP signaling in antiviral defense and immune adjuvant effects. Science 341: 1390-1394. doi:10.1126/science.1244040. PubMed: 23989956.
40. Oshiumi H, Matsumoto M, Hatakeyama S, Seya T (2009) Riplet/RNF135, a RING finger protein, ubiquitinates RIG-I to promote interferon-beta induction during the early phase of viral infection. J Biol Chem 284: 807-817. PubMed: 19017631.
41. Oshiumi H, Miyashita M, Inoue N, Okabe M, Matsumoto M et al. (2010) The ubiquitin ligase Riplet is essential for RIG-I-dependent innate immune responses to RNA virus infection. Cell Host Microbe 8: 496-509. doi:10.1016/j.chom.2010.11.008. PubMed: 21147464.

Research Article

Journal of Innate Immunity

J Innate Immun
DOI: 10.1159/000355126

Received: August 12, 2013
Accepted after revision: August 19, 2013
Published online: October 29, 2013

Myeloid-Derived Suppressor Cells Confer Tumor-Suppressive Functions on Natural Killer Cells via Polyinosinic:Polycytidylic Acid Treatment in Mouse Tumor Models

Hiroaki Shime Ayako Kojima Akira Maruyama Yusuke Saito
Hiroyuki Oshiumi Misako Matsumoto Tsukasa Seya

Department of Microbiology and Immunology, Graduate School of Medicine, Hokkaido University, Sapporo, Japan

Key Words
Myeloid-derived suppressor cells · Mitochondrial antiviral signaling protein · Tumor immunotherapy · Double-stranded RNA

Abstract
Polyinosinic:polycytidylic acid (poly I:C), a synthetic double-stranded RNA, acts on myeloid cells and induces potent antitumor immune responses including natural killer (NK) cell activation. Myeloid-derived suppressor cells (MDSCs) systemically exist in tumor-bearing hosts and have strong immunosuppressive activity against antitumor effector cells, thereby dampening the efficacy of cancer immunotherapy. Here we tested what happened in MDSCs in poly I:C-treated mice. NK-sensitive syngenic tumor (B16)-bearing C57BL/6 mice were employed for this study. Intraperitoneal poly I:C treatment induced MDSC activation, driving CD69 expression and interferon (IFN)-γ production in NK cells. IFN-γ directly inhibited proliferation of B16 cells. This NK cell priming led to growth retardation of B16 tumors, although no direct tumoricidal activity was induced in NK cells. Mechanistic analysis using KO mice and function-blocking monclonal antibody revealed that MDSCs produced IFN-α via the mitochondrial antiviral signaling protein (MAVS) pathway after in vivo administration of poly I:C, and activated NK cells through the IFNAR pathway. MDSC-mediated NK cell priming was reconstituted by IFN-α in a coculture system. Either the MAVS or IFNAR signaling pathway was required for activation of MDSCs that led to growth retardation of B16 tumor in vivo. The results infer that MDSC is a target of poly I:C to prime NK cells, which exert antitumor activity to NK-sensitive tumor cells.

Introduction

The innate sensing of microbial molecular patterns results in the modulation of the cellular immune system [1–3]. This innate-adaptive linkage closely associates with suppression of infection and tumorigenesis. Many reports showed that polyinosinic:polycytidylic acid (poly I:C), a synthetic pattern of double-stranded RNA, has potent stimulatory effects on immune responses to viral infection and cancer [4–8]. Poly I:C is an agonist for pattern-recognition receptors (PRRs), Toll-like receptor 3 (TLR3) and melanoma differentiation-associated protein 5 (MDA5), which transduce signals to the adaptor molecules TICAM-1 (also known as TRIF) and mitochondrial antiviral signaling protein (MAVS; IPS-1, Cardif, VISA) [9–12]. They differentially modulate the functions of myeloid dendritic cells (DCs) and macrophages, including cytokine/IFN production and expression of surface molecules that drive effector cell activation.

KARGER

E-Mail karger@karger.com
www.karger.com/jin

1662–811X/13/0000–0000$38.00/0

Dr. Tsukasa Seya and Dr. Hiroaki Shime
Department of Microbiology and Immunology
Graduate School of Medicine, Hokkaido University
Kita-ku, Sapporo 060-8638 (Japan)
E-Mail seya-tu@pop.med.hokudai.ac.jp and shime@med.hokudai.ac.jp

TLR3/TICAM-1 and MDA5/MAVS activate the transcription factors, NF-κB and interferon (IFN) regulatory factor 3 (IRF-3), to typically induce type-I IFN. Type-I IFN evokes subsequent activation of the IFNAR pathway, which participates in the induction of IFN-stimulated genes (ISGs) including IRF-7 [13, 14]. IRF-7 further modifies the function of poly I:C by upregulating PRRs. Thus, the activity of poly I:C immediately affects IRF-3-derived genes and secondarily upregulates genes by activation of the IFNAR pathway. These pathways are crucial for driving the effector functions of NK cells and cytotoxic T cells that result in tumor regression after poly I:C treatment [6, 15].

NK cells are important for antitumor effects not only through direct cytotoxic activity, but also indirectly, through the production of cytokines including IFN-γ [16–20]. $DX5^+$ or $NK1.1^+$ cells have been used as conventional NK cells, which have features distinct from other lymphoid cells. Optimal NK cell responses require the presence of accessory cells such as DCs or macrophages [21]. NK cells are essential for poly I:C-induced growth retardation of NK-sensitive tumors such as B16 melanomas since poly I:C treatment does not induce antitumor activity in NK cell-depleted mice [4, 5]. IFN-γ production and cytotoxic activity by NK cells are potentiated by stimulating mice in vivo with poly I:C. NK cell activation appears to have many modes and myeloid NK cell contact serves a critical factor for antitumor NK cell activation.

Myeloid-derived suppressor cells (MDSCs) belongs to myeloid lineages with potent immunosuppressive activity against antitumor immune responses in mice and humans [22, 23]. MDSCs are widely distributed at tumor sites and in the peripheral organs, spleen and lymph nodes. Defined as a $CD11b^+Gr1^+$ subset in mice, they are heterogeneous populations of early myeloid progenitors that arise in bone marrow. Recently, they have also been found to originate from hematopoietic stem and progenitor cells accumulated in the spleen under tumor-bearing conditions [24]. The immunoregulatory functions of MDSCs in cancer have been studied extensively [22, 25]. MDSCs inhibit antigen-dependent T cell proliferation through the production of immunosuppressive factors including arginase-1, reactive oxygen species and reactive nitrogen species, and the release of immunosuppressive cytokines. However, the effect of MDSCs on NK cell function in tumor-bearing hosts is controversial. The anergy of NK cells is reportedly induced by MDSCs through membrane-bound TGF-β in a tumor-implant model using 3LL, B16 and EG7 cells [26]. MDSCs derived from patients with hepatocellular carcinoma inhibit autologous NK cell activity when cocultured in vitro [27]. Splenic MDSCs in TS/A tumor-bearing mice repress NK cell cytotoxicity [28]. A subset of MDSCs expresses NKG2D ligand on the cell surface and activates NK cells through NKG2D-NKG2D ligand interaction [29]. Although MDSCs express PRRs, their contribution to the MDSC function in poly I:C-induced growth retardation of tumors has not been fully understood.

Recent studies have demonstrated that TLR stimulation could modulate the function of immunosuppressive myeloid-derived cells as well as myeloid DCs in cancer. Tumor-associated macrophages and MDSCs were converted from tumor supporters to tumoricidal effectors after treatment with TLR agonists [7, 30, 31]. It was demonstrated that CpG treatment blocks MDSC-mediated T cell suppression associated with the maturation and differentiation of MDSCs [30, 31]. In this study, we revealed that poly I:C treatment allows cancer-expanded MDSCs to prime NK cells through the MAVS and the type-I IFN signaling pathway in vivo, leading to retardation of tumor growth.

Materials and Methods

Mice and Tumor Cells

Inbred C57BL/6 wild-type (WT) mice were purchased from Clea, Japan. $TICAM\text{-}1^{-/-}$ and $MAVS^{-/-}$ mice were generated in our laboratory. $IFNAR1^{-/-}$ mice were kindly provided by T. Taniguchi (University of Tokyo). Mice of 6- to 10-weeks of age were used in all experiments that were performed according to animal experimental ethics committee guidelines of Hokkaido University. B16D8 cells were developed in our laboratory [4]. B16D8 cells were cultured at 37°C under 5% CO_2 in RPMI containing 10% FBS, penicillin and streptomycin. This study was carried out in strict accordance with the recommendations in the Guide for the Care and Use of Laboratory Animals of the National Institutes of Health (USA). The protocol was approved by the Committee on the Ethics of Animal Experiments in the Animal Safety Center, Hokkaido University, Japan. All mice were used according to the guidelines of the institutional animal care and use committee of Hokkaido University, who approved this study as ID number 08-0290, 'Analysis of Anti-Tumor Immune Response Induced by the Activation of Innate Immunity'.

Tumor Challenge and Poly I:C Treatment

Mice were shaved at the back and injected s.c with B16D8 cells (6×10^5), 3LL cells (3×10^6) or EL4 cells (1×10^6) suspended in 200 μl PBS(–). Tumor size was measured using a caliper. Tumor volume was calculated using the following formula: tumor volume (cm^3) = (long diameter) × (short diameter)^2 × 0.4. Poly I:C (GE Bioscience) (200 μg/head) with no detectable LPS was injected i.p. as indicated. In some cases, polymixin B-treated poly I:C was used. When an average tumor volume of 0.4–0.6 cm^3 was reached, the treatment was started and was repeated every 4 days.

Cell Isolation and Culture

When tumor volume reached 1–2 cm^3, i.e. 14–18 days after tumor challenge, mice were injected i.p. with 200 μg poly I:C or PBS(–). After 4 h, $CD11b^+Gr1^+$ MDSC-like cells were isolated from splenocyte suspension or single-cell suspension from the collagenase-treated tumor of poly I:C-injected or PBS-injected mice by using biotin-conjugated anti-Gr1 monoclonal antibody (RB6–8C5) and Streptavidin Microbeads (Miltenyi) as described previously [7]. NK cells were purified from splenocytes of naïve mice by using DX5 Microbeads (Miltenyi). In these purification steps, two rounds of positive selection were performed. We routinely prepared $Gr1^+$ cells at more than 95% purity and almost 100% of $Gr1^+$ cells expressed CD11b. The purity of $DX5^+$ cells was more than 90%. Isolated $CD11b^+Gr1^+$ cells and $DX5^+$ cells were cocultured for 20–24 h. In some experiments, anti-IFNAR1 monoclonal antibody (MAR1–5A3) was added to the culture for neutralization of IFNAR1. Recombinant mouse IFN-α (R&D systems) was used for stimulation of $CD11b^+Gr1^+$ cells and NK cells.

Cells isolated from mouse spleen were incubated for 24 h and the conditioned medium was collected. Concentrations of IFN-α and IFN-γ were determined by ELISA according to manufacturer's instructions (PBL Interferon Source and eBioscience). NK cytotoxicity was determined by standard ^{51}Cr release assay as described previously [32].

Flow Cytometric Analysis

Mononuclear cells prepared from mouse spleen or tumor were treated with anti-CD16/32 (no. 93) and stained with FITC- or APC-anti-CD45.2 (no. 104), FITC- or PE-anti-CD11b (M1/70), APC- or PE-anti-GR1 (RB6–8C5), PE- or APC-anti-NK1.1 (PK136), PE-anti-CD49b (DX5), FITC-, PE- or APC-anti-CD3ε (145–2C11), FITC- or PE-anti-CD69 (H1.2F3), PE-anti-CD80 (16–10A1), PE-anti-CD86 (GL-1), PE-anti-CD40 (1C10), PE-anti-CD155 (TX56), PE-anti-CD70 (FR70), PE-anti-IL-15Ra (DNT15Ra), FITC-anti-CD150 [A12 (7D4)], and anti-RAE-1 (eBioscience and Biolegend). Samples were analyzed with a FACSCalibur instrument or FACS Aria instrument (BD Bioscience) and data analysis was performed by FlowJo software (Tree Star).

T Cell Proliferation Assay

T cell proliferation was measured by changes in fluorescence intensity using carboxyfluorescein diacetate succinimidyl ester (CFSE). Splenocytes from OT-I transgenic mice were labeled with 1 μM CFSE, placed into a round bottom 96-well plate containing $CD11b^+Gr1^+$ cells as indicated. Splenocytes were cultured in the presence of 100 nM OVA-derived peptide SIINFEKL. After 3 days, cells were harvested, stained with APC-anti-CD8α (53–6.7) and PE-anti-TCR vβ 5.1, 5.2 (MR9–4) or PE-anti-CD3ε (145–2C11), and the CFSE signal of gated lymphocytes was analyzed by flow cytometry. The extent of cell proliferation was quantified by FlowJo software (Tree Star).

Quantitative PCR Analysis

RNA was prepared with RNeasy kit (QIAGEN) or TRIZOL reagent (Invitrogen) according to the manufacturer's instruction. Reverse transcription was performed using High-Capacity cDNA Reverse Transcription kit (Applied Biosystems). Real-time PCR was performed with Power SYBR Green PCR Master Mix (Applied Biosystems) with StepOne™ Real-time PCR system (Applied Biosystems). Expression of the cytokine gene was normalized to the expression of glyceraldehyde phosphate dehydrogenase (GAPDH). The following primers were used for PCR: IFNα4 forward, 5′-CTGCTGGCTGTGAGGACATACT-3′, IFNα4 reverse, 5′-AGGCACAGAGGCTGTGTTTCTT-3′, IL-15 forward, 5′-TTAACTGAGGCTGGCATTCATG-3′, IL-15 reverse, 5′-ACCT ACACTGACACAGCCCAAA-3′, IL-18 forward, 5′-GACAAA GAAAGCCGCCTCAA-3′, IL-18 reverse, 5′-ATGGCAGCCAT TGTTCCTG-3′, INAM forward, 5′-CAACTGCAATGCCACG CTA-3′, INAM reverse, 5′-TCCAACCGAACACCTGAGACT-3′, GAPDH forward, 5′-GCCTGGAGAAACCTGCCA-3′, GAPDH reverse, 5′-CCCTCAGATGCCTGCTTCA-3′. Data was analyzed by the ΔΔCt method.

Statistics

If not otherwise stated, data were expressed as arithmetic means ± SD, and statistical analyses were made by 2-tailed Student's t test. $p < 0.05$ was considered statistically significant.

Results

$CD11b^+Gr1^+$ Cells Expanded in B16 Tumor-Bearing Mice Are Immunosuppressive

$CD11b^+Gr1^+$ cells representing MDSCs accumulate in large numbers in the lymphoid tissues of tumor-bearing mice [22, 23]. We therefore investigated the spleens of mice bearing syngenic tumor cells. B16 melanoma cells, 3LL lung cancer cells or EL4 thymoma cells were s.c. injected into WT mice and, 16 days later, splenic populations of immune cells were examined in the tumor-bearing mice. The proportion of $CD11b^+Gr1^+$ cells in the spleens of B16-implanted mice was higher than that in tumor-free naïve mice, consistent with previous reports (fig. 1a). Similar profiles were obtained with the 3LL and EL4 cell lines (data not shown).

To examine whether $CD11b^+Gr1^+$ cells had immunosuppressive activity, we harvested $CD11b^+Gr1^+$ cells from the spleens of B16 tumor-implanted mice, and cocultured $CD11b^+Gr1^+$ cells with OT-I splenocytes in the presence of OVA peptide. $CD11b^+Gr1^+$ cells from tumor-bearing mice efficiently inhibited antigen-specific proliferation of $CD8^+$ OT-I T cells (fig. 1b). Therefore, $CD11b^+Gr1^+$ cells accumulated in the spleen of B16 tumor-bearing mice and had immunosuppressive functions.

We also assessed the immunosuppressive activity of $CD11b^+Gr1^+$ cells against NK cells activated by PMA/ionomycin and tested activation as level of IFN-γ production. No inhibitory effect of $CD11b^+Gr1^+$ cells on the production of IFN-γ by NK cells was observed (online suppl. fig. 1; for all online suppl. material, see www.karger.com/doi/10.1159/000355126). Therefore, $CD11b^+Gr1^+$ cells expanded in B16 tumor-bearing mice exhibited immunosuppressive activity toward $CD8^+$ T cells but not NK cells.

In vivo Poly I:C Induces Cytokine Production and Maturation of CD11b⁺Gr1⁺ Cells

Type-I IFNs are systemically produced in tumor-bearing mice by i.p. injection of poly I:C. Poly I:C usually acts on TLR3 in myeloid/epithelial cells and MDA5 in systemic cells, leading to type-I IFN production [33]. Since CD11b⁺Gr1⁺ cells expressed both TLR3 and MDA5, we examined whether type-I IFNs were produced by CD11b⁺Gr1⁺ cells in B16 tumor-bearing mice in response to poly I:C injection. Interestingly, we found that IFN-α is produced in splenic CD11b⁺Gr1⁺ cells harvested from poly I:C-treated B16 tumor-bearing mice, but not in CD11b⁺Gr1⁺ cells unexposed to poly I:C (fig. 2a, left panel). The results were also confirmed in vitro: type-I IFNs was minimally produced in poly I:C-untreated CD11b⁺Gr1⁺ cells but robustly in poly I:C-treated cells from the spleen or tumor in direct response to poly I:C (fig. 2a, right panel). The results were reproducible with different tumor cell lines, specifically 3LL and EL4, and different sources of CD11b⁺Gr1⁺ cells

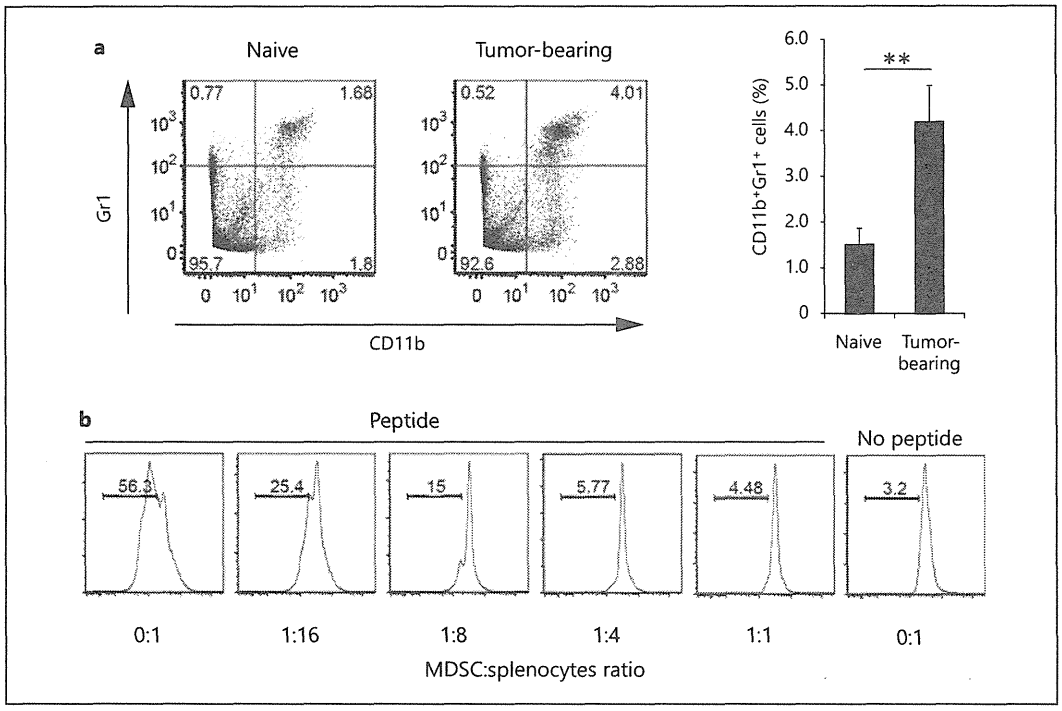

Fig. 1. Immunosuppressive activity of CD11b⁺Gr1⁺ cells in the spleen of B16 tumor-bearing mice. **a** WT mice were injected s.c. with B16D8 melanoma cells. The percentage of CD11b⁺Gr1⁺ cells in the spleen was determined on day 16 by flow cytometry (n = 6). Cells were gated on CD45⁺ cells. **b** CD11b⁺Gr1⁺ cells were isolated from spleens of B16 tumor-bearing mice, and cultured with CFSE-labeled OT-I splenocytes (1×10^6) at the indicated ratios. After 3 days, proliferation of CD8α⁺TCRvβ⁺ cells was measured. Data shown are representative of at least 2 independent experiments. ** $p < 0.01$.

Fig. 2. Effect of poly I:C treatment on CD11b⁺Gr1⁺ cells. **a** B16 tumor-bearing mice were injected i.p. with 200 μg poly I:C or PBS as a negative control. After 4 h, CD11b⁺Gr1⁺ cells were purified from spleens and incubated for 24 h (left panel). CD11b⁺Gr1⁺ cells isolated from spleens of B16 tumor-bearing mice were treated with 50 μg/ml poly I:C or PBS for 24 h (right panel). The concentration of IFN-α in conditioned medium was determined. **b** 3LL cells (3×10^6) were implanted into B6 WT mice and CD11b⁺Gr1⁺ cells were isolated from spleen (left panel) or tumor (right panel) after poly I:C injection as described in **a**. **c** Spleen cells were prepared from B16 tumor-bearing mice treated with poly I:C or PBS for 8 h as described in **a** and surface expression of CD80, CD86, CD40, RAE-1, CD155, CD70, IL-15RA and CD150 on CD11b⁺Gr1⁺ cells was determined. **d** CD11b⁺Gr1⁺ cells were isolated from B16 tumor-bearing mice treated with poly I:C or PBS for 4 h as described in **a** and mRNA for IFN-α4, IL-15, IL-18, INAM and arginase-1 was measured (n = 3). Data shown are representative of at least 2 independent experiments. ** $p < 0.01$, * $p < 0.05$. NS = Not significant.

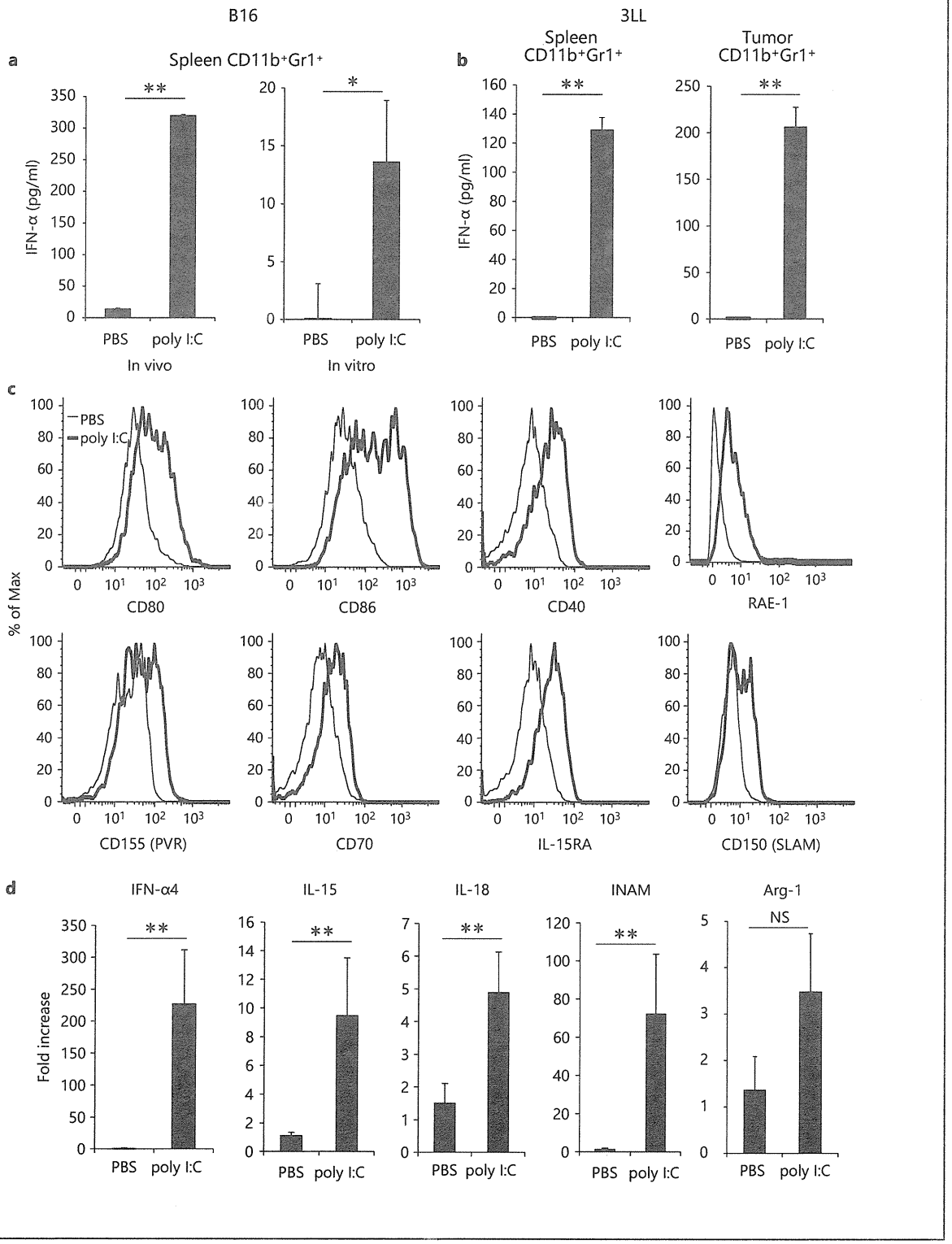

2

(fig. 2b; online suppl. fig. 2a). In addition, the costimulatory molecules CD80 and CD86 on these cells were upregulated in response to poly I:C (fig. 2c). To further investigate the effect of poly I:C treatment on the function of $CD11b^+Gr1^+$ cells, we analyzed the gene expression of $CD11b^+Gr1^+$ cells isolated from B16 tumor-bearing mice, 4 h after injection with poly I:C or PBS. We found an increase in mRNA for IFN-α4, IL-15, IL-18 and INAM (fig. 2d) [21, 32]. Furthermore, in vivo poly I:C treatment for 8 h resulted in upregulation of RAE-1, PVR (CD155), CD70, IL-15RA, SLAM (CD150) and CD40 on $CD11b^+Gr1^+$ cell surface (fig. 2c). These molecules are involved in DC-mediated NK cell activation [18, 34, 35]. However, mRNA for arginase-1, which is involved in MDSC-mediated inhibition of T cell proliferation, was not increased in $CD11b^+Gr1^+$ cells (fig. 2d). These results suggest that in vivo pretreatment of mice with poly I:C effectively induces the maturation of $CD11b^+Gr1^+$ cells, resulting in enhanced expression of NK cell-activating molecules.

$CD11b^+Gr1^+$ Cells from Poly I:C-Treated Tumor-Bearing Mice Activate NK Cells

To investigate whether $CD11b^+Gr1^+$ cells from poly I:C-injected tumor-bearing mice are capable of activating NK cells, we isolated $CD11b^+Gr1^+$ cells from the spleens of tumor-bearing mice after poly I:C administration and cocultured the cells with NK cells from naïve mice. NK cells upregulated CD69 on their surface in response to the $CD11b^+Gr1^+$ cells from poly I:C-injected B16 tumor-bearing mice. However, the level of CD69 on NK cells was not changed when the cells were mixed with $CD11b^+Gr1^+$ cells from PBS-injected tumor-bearing mice (fig. 3a, left panel). $CD11b^+Gr1^+$ cells from poly I:C-injected tumor-bearing mice also induced NK cell IFN-γ production (fig. 3a, right panel). Similar results were obtained with NK cells cocultured with $CD11b^+Gr1^+$ cells from mice bearing 3LL- or EL4 cell tumors after poly I:C treatment (fig. 3b, c; online suppl. fig. 2b, c). Furthermore, $CD11b^+Gr1^+$ cells from tumors of 3LL-implant mice had a similar ability to induce IFN-γ production and CD69 expression in NK cells after poly I:C treatment (fig. 3c). IFN-γ inhibits proliferation of B16 cells in vitro without affecting the cell viability (online suppl. fig. 3; data not shown). In contrast, $CD11b^+Gr1^+$ cells did not drive a cytotoxic phenotype from NK cells (fig. 3d). In vitro stimulation of $CD11b^+Gr1^+$ cells with poly I:C did not induce NK cytotoxicity in coculture (data not shown). These results demonstrated that when poly I:C was injected into tumor-bearing mice, $CD11b^+Gr1^+$ cells acquired the ability to prime NK cells as measured by CD69 expression and IFN-γ production, but did not induce cytotoxic activity.

Type-I IFN Signaling Is Essential for NK Cell Priming by $CD11b^+Gr1^+$ Cells

Next, we investigated the mechanisms by which $CD11b^+Gr1^+$ cells primed NK cells through the in vivo administration of poly I:C. Soluble factors and membrane-associated molecules induced by poly I:C are reportedly involved in in vivo NK cell activation [15, 18]. As shown in figure 2a, $CD11b^+Gr1^+$ cells from poly I:C-treated tumor-bearing mice produced IFN-α. To examine whether type-I IFN signaling through IFNAR was involved in NK cell activation, we added anti-IFNAR1 antibodies to cultures to inhibit type-I IFN signaling by both $CD11b^+Gr1^+$ and NK cells that express IFNAR1. CD69 upregulation on NK cells and IFN-γ production induced by activated $CD11b^+Gr1^+$ cells were completely abrogated by anti-IFNAR1 antibodies (fig. 4a). These results suggest that type-I IFN signaling is essential for NK cell priming by $CD11b^+Gr1^+$ cells.

To investigate type-I IFN signaling in NK cell priming, we prepared NK cells from $IFNAR1^{-/-}$ mice. $IFNAR1^{-/-}$ NK cells were cocultured with $CD11b^+Gr1^+$ cells. $CD11b^+Gr1^+$ cells from poly I:C-stimulated WT mice stimulated CD69 expression and IFN-γ production by WT NK cells but not $IFNAR1^{-/-}$ NK cells (fig. 4b). Therefore, type-I IFN signaling in NK cells is essential for NK priming by $CD11b^+Gr1^+$ cells.

To examine whether IFNAR signaling is the only route for the induction of $CD11b^+Gr1^+$ cell-mediated NK priming, we added recombinant mouse IFN-α to cultures of NK cells or to cocultures of untreated $CD11b^+Gr1^+$ cells and WT NK cells. Recombinant mouse IFN-α in NK cell cultures resulted in induction of CD69 expression on the NK cells (fig. 4c, left panels). However, CD69 expression was minimally augmented in the NK cells cocultured with $CD11b^+Gr1^+$ cells. In contrast, NK cell IFN-γ production was clearly induced at high concentrations of IFN-α (2,000 IU/ml) and augmented by $CD11b^+Gr1^+$ cells (fig. 4c, right panel).

We investigated if cell-cell contact is involved in NK cell activation in cocultures of $CD11b^+Gr1^+$ cells and naïve NK cells using the Transwell system. Sufficient NK cell priming was detected when NK cells were cocultured with in vivo poly I:C-activated $CD11b^+Gr1^+$ cells. However, expression of CD69 and production of IFN-γ by NK cells was abrogated by separation of the cells by the Transwell membrane (online suppl. fig. 4a, b). These results,